2023. Journal of Arachnology 51:123–138

Postembryonic development in pseudoscorpions: allometry in *Geogarypus italicus* (Pseudoscorpiones: Geogarypidae)

Matteo Zinni[1], **Giulio Gardini**[2] and **Loris Galli**[1]: [1]DISTAV, Genoa University, Corso Europa 26, 16132 Genoa, Italy. E-mail: matteo.zinni89@gmail.com; [2]Via Monte Corno 12/1, 16166 Genoa, Italy.

Abstract. Pseudoscorpions are arachnids featuring three nymphal instars before reaching the adult age. Instars can be mostly recognized based on the number of trichobothria which lie along the chelal axis: as the individual grows, further trichobothria are added. The study of the post-embryonic growth based on trichobothria position has been the most widely used approach. However, other body parts can be subjected to particular growth patterns that need to be explored to fully understand post-embryonic development processes. Rigorous numerical approaches that allow meaningful statistical inference within growth regressions are now available. The recently described Mediterranean species *Geogarypus italicus* Gardini, Galli & Zinni, 2017 gave the authors the chance to review studies carried out in the past with the modern statistical approach mentioned above. Results confirm the main hypothesis about the growth process of the chelal axis but showed some differences that may be related to taxonomical aspects. Moreover, the study of body allometry during post-embryonic growth showed that not all body parts undergo the same trend from protonymphs to males, on one side, and to females, on the other. Finally, the study of proportions between body parts through the analysis of ratios between their linear measurements pointed out a marked sexual dimorphism of pedipalps in spite of similar sizes and proportions of other body regions. The analysis led us to think that more interesting information could come from applying this approach to multispecies studies.

Keywords: Allometric growth, Italy, nymphal instars, sexual dimorphism, trichobothria

https://doi.org/10.1636/JoA-S-21-075

Life history studies aim to describe the series of changes that a species undergoes during its whole life cycle. In contrast to better studied arachnids, such as scorpions and spiders, life histories of the minor arachnid groups like pseudoscorpions are only known from few studies and often limited to qualitative aspects and descriptive considerations because of several difficulties, such as the efficient sampling of individuals (Gabbutt 1970a). The recent addition of *Geogarypus italicus* Gardini, Galli & Zinni, 2017 by Gardini et al. (2017) to the European fauna, thanks to the large number of specimens available, represents a unique opportunity to study the post-embryonic development of pseudoscorpions using a rigorous statistical framework that may deliver important results to assess differences among post-embryonic instars and sheds light into the growth patterns of these small arachnids. The existence of growth centers and growth gradients in arthropod appendages was first recognized by Huxley (1932). Particular emphasis in describing these processes has been put to solve allometry-related problems. Allometry can be defined in its simplest formulation as the set of differences in proportions correlated (positively or negatively) with changes in absolute size of the total organism or of the specific body part (Gould 1966). It can be mathematically described as a regression of the size of one part itself or in proportion to the size of another (Reiss 1991). Differential scaling of individual body parts is the result of selection that could lead either to exaggerated (positive allometry) or reduced (negative allometry) size, whereas other parts may remain proportionally unmodified (isometry) (Fox et al. 2015). This relationship has been widely used both under the static (Shingleton 2010) and the ontogenic (Shea 1985) perspectives to investigate several aspects of arachnid orders such as sexual dimorphism (McLean et al. 2018) and growth processes (Gnaspini 1995). Within pseudoscorpions, the pedipalpal chela is without any doubt one of the most investigated structures. Since Vachon (1936) documented the post-embryonic changes in pseudoscorpion trichobothrial number, which led to the identification of the four post-embryonic instars, the study of chelal growth became the main focus of interest.

Protonymphs bear an initial set of 4 trichobothria. During the growth process four trichobothria, *it*, *est*, *ib* and *b*, are added in the deutonymph. Two trichobothria, *st* and *esb*, are added in the tritonymph. With few exceptions that occur in the Menthidae and Ideoroncidae families (Harvey 1992), the full complement of twelve trichobothria is achieved by the appearance of *isb* and *sb* in adults. Despite this growth, the initial and final position of *it*, in the protonymph and in the adult respectively, remains almost the same.

Gabbutt and Vachon were the first who explored chelal allometry (Gabbutt & Vachon 1965, 1967; Gabbutt 1969, 1972), followed by only two studies by Sivaraman (1982) and Gardini & Benelli (1991). Studies related to other body parts are even more rare and mostly focused on addressing sexual dimorphism (Zeh 1987; Palen-Pietri et al. 2019), despite the fact that many body features could potentially yield interesting information (Harvey 1987, 1988). Therefore, the analysis of the growth process in pseudoscorpions should not be only limited to pedipalpal chela.

In the morphometric approach to the study of animals and their growth, the analysis of ratios between linear measurements has a long tradition in taxonomy (Blackith & Reyment 1971; Winston 1999) where they have been used in species descriptions, diagnoses, or identification keys (Mayr & Ashlock 1991). In the current study, the authors adopted a modern statistical approach, based both on linear measurements and some ratios of *Geogarypus italicus* among those

traditionally used by the specialists of the group in order to pursue the following objectives: (i) test the hypothesis initially formulated by Gabbutt (1969) about the changes of the relative position among trichobothria during the growth process and how it occurs along the chelal axis (Gabbutt 1965) during post-embryonic development; (ii) assess the possibility to predict chelal growth based on trichobothrial position in each instar; (iii) investigate the size increment of all body parts to describe potential patterns of ontogenetic allometry (Klingenberg & Zimmermann 1992); and (iv) describe the change in terms of proportions and shape that occur from protonymph to adults in *G. italicus*.

METHODS

In order to describe the post-embryonic growth of *G. italicus,* 50 specimens – 10 for each instar and for both sexes – were examined. Material was derived from the type locality at Bergeggi (Savona province, North West Italy, 44°15′27″N, 8°26′35″E), from soil on cork oak (*Quercus suber*) wood.

Specimens were cleared in 10% KOH solution at 40°C for several hours, washed in distilled water and temporarily mounted—after dissection of right palp, chelicera, legs I and IV—in cavity slides with 60% lactic acid. After study each specimen was rinsed in distilled water and returned to a vial of 70% ethanol together with the dissected portions in glass capillary tubes. Drawings were made using an Olympus BHB compound microscope with the aid of a Nachet drawing tube. Measurements (expressed in mm) were taken with the aid of an interference contrast microscope (Leica DM LB2), a Leica DFC 295 camera and Leica Application Suite Vers. 3.8. In particular, the following set of characters was measured. Carapace: carapace length and width, cucullus length, carapace furrow. Chelicera: chelicera length, chelicera width and chelicera movable finger length. Pedipalps: trochanter length, trochanter width, femur length, femur width, patella length, patella width, chela with pedicel length, chela without pedicel length, hand with pedicel width, hand length without pedicel, hand width, movable finger length. Moreover, the distance of each trichobothrium from the tip of the chela was measured along the chelal axis (Gabbutt 1965) following the approach proposed by Gabbutt (1969). Leg I and Leg IV: trochanter length and depth, femur length and depth, patella length and depth, tibia length and depth, basitarsus length and depth, telotarsus length and depth. Ratios between measurements were calculated as length/width for carapace, chelicerae and pedipalps and as length/depth for legs.

The terminology adopted follows Chamberlin (1931), Gabbutt (1972) and Gardini & Benelli (1991). In this work the term instar has been applied in its usual definition to identify the developmental phase between two molts (Canard & Stockman 1993), while stage is used when a pair of successive instars are considered. For stages, the following abbreviations were used: PD = protonymph to deutonymph, DT = deuto- to tritonymph, TM = tritonymph to male, and TF = tritonymph to female. In order to make our results comparable with past works, four decimal places have been considered.

Analyses were performed within R environment (R core Team 2017) using smatr (Warton et al. 2012), lawstat (Hui et al. 2008), PMCMR (Pohlert & Pohlert 2018) and MASS (Ripley et al. 2013) packages. Smatr allows better line fitting and estimation through standardized major axis regression with a robust Huber's M estimation, very suitable in allometry and growth studies. Axis growth lines and all regression lines fitted to linear measurements were tested against the null hypothesis of isometry and their slopes studied through pairwise comparison with p-value adjustment (Sidak adjustment) to control group-wise error rate in a conservative way. Graphical output was provided via ggplot2 (Wickham 2011).

Testing trichobothria positions.—Since trichobothria appear sequentially, it is possible to quantify the "movement of each of them" during the post embryonic process by simply subtracting their distance from the tip of the chela from that measured in the previous instar: negative values will describe a movement toward the tip in contrast with positive values that will outline a shift to a more basal position along the chela (following Gabbutt (1969), Gardini and Benelli (1991)).

The mean values of distance from the finger-tip and trichobothrial mean ratios (i.e., the ratio between the distance of each trichobothrium from the finger-tip and the length of chelal axis according Gabbutt 1970b) of each trichobothrium were tested with a significance level of 0.05 against the null hypothesis that no modification occurs during growth. When data met the assumptions of normality and homoschedasticty, a one-way Anova was used, otherwise a Kruskal-Wallis test was applied. Tukey's HSD and Dunn's Test (Dunn 1961) were used to perform pairwise comparisons.

Chelal axis growth.—The chelal axis in protonymph, deutonymph, tritonymph, male and female are represented by b_0, b_1, b_2, b_3, and b_4 respectively. The change in the length of the chelal axis from an instar to the following one is described by a line drawn from origin to the point $(b_{(n-1)}, b_{(n)})$. To infer growth between successive instars, an analysis of covariance (sensu Sokal & Rohlf 1995) was run to test the slope of the lines against the null hypothesis of isometric growth described by a line with a slope equal to 1 and that of a constant growth with the same slope along the whole post-embryonic process (Warton & Weber 2002).

Growth models.—The original formulation provided by Gabbutt (1969) was used to fit models within *G. italicus* trichobothrial data. The distance from the distal end of the chelal axis of each trichobothrium for each instar (a_n) was plotted against the same distance in the previous instar (a_{n-1}). A bivariate regression described by the equation $y = mx + c$, where the slope "m" represents the relationship $a_{(n)}/a_{(n-1)}$, was fitted to trichobothrial data (Gabbutt 1970b). As reported in Gabbutt (1969), the amplitude of the growing region can be estimated by calculating the intersection of the regression line fitted between trichobothria with two other lines. The distal end of this portion (middle growing region) is obtained by intersecting the previously mentioned regression line ($y = mx + c$) with the $y = x$ line, under the assumption that no growth occurs in the distal part of the axis. The proximal limit of this growing region is achieved by intersecting the trichobothrial regression with the line with slope equal to one and traced from the point having coordinates $(b_{(n-1)}, b_{(n)})$. Thus, the reliability of the formula provided by Gabbutt (1972) to predict the position of trichobothria in each instar was verified through a Wilcoxon non-parametric test adjusted for paired data. For the regression fitted between deutonymphal and tritonymphal trichobothria, the distal intersection with $y = x$

line falls over the end of the chelal axis: to overcome this eventuality the absence of a proximal non-growing region was considered as proposed by Gabbutt (1972). The value of males was recalculated under the assumption that the trichobothrial and chelal regressions coincide at a point equal to the length of the chelal axis.

Growth rates and increments.—For all couples of subsequent instars (namely stages), it is possible to calculate the distances between the tip of the chelal axis and the most distal trichobothrium, between pairs of contiguous trichobothria along the whole axis and finally between the most proximal trichobothrium and the base of the fixed finger. Thus, the difference between the distances of two successive trichobothria in two following stages represents their linear increment. The distance between two successive trichobothria in one stage divided by their distance in the previous stage gives a value for the growth rate of a specific section along the chelal axis. The calculated values were plotted as follows. Along the horizontal axis, the distances from the tip of chela of trichobothria and base was shown to represent the increment along the chelal axis in the previous stage. On the vertical axis the growth rate of each portion across two following instars was represented. The middle growing region (see the previous paragraph) was highlighted as a grey rectangle for which base and height are the interval between its proximal and distal ends, and its growth rate, respectively (Fig. 36).

Size and proportions.—The fluid permeation through tissues during the preparation/clearing phases and the behaviour of lateral pleurae can cause the compression and dilation of the whole opisthosoma. For this reason, body length cannot be considered a reliable proxy measurement to study allometry since it could lead to misleading measurements. Carapace length (Cl) could represent a good choice to describe allometry within measured specimens, being a unique piece that is strongly sclerified (Zeh 1987; McLean et al. 2018). Multiple bivariate regressions were fitted between Cl (independent variables) and the lengths of other body parts to study ontogenetic allometry. In order to extend the current model to include other species, the length of the cucullus has been deducted from the actual carapace length. To better understand and concurrently compare growth patterns, body features used in linear models as explanatory variables have been grouped into four areas. The upper body region (UB) includes chelicera length and the length of the movable finger. Features belonging to pedipalps and chela (PC) are: trochanter length, femur length, patella length, chela with pedicel length, chela without pedicel length and movable finger length. Leg I (LI) and leg IV (LIV) both include trochanter length, femur length, patella length, patella depth, tibia length, basitarsus length, telotarsus length and telotarsus depth. Regressions were fitted separately to male and female data to explore differences in the growth processes; to avoid trivial results, multicollinear measurements such as length of cheliceral movable finger, length of chela without pedicel, hand with pedicel width, hand without pedicel length and movable finger length have been discarded from models.

Ratios are commonly used to quantify the shape of organisms; similarity or dissimilarity in proportions of two specimens can be translated then into a series of ratios that help the taxonomist to discriminate between species (Baur & Leuenberger 2011). One of the most used analyses within this field is Fisher's linear discriminant analysis (LDA), which aims to find linear combinations of features that separate two or more groups into a dimensionally reduced space described by a new system of coordinate axes. To look at how ratios obtained by dividing the length of each feature by its width, define specific patterns of growth and shape variations within instars, four multiple linear discriminant analysis, one for each body area defined above (UB, PC, LI and LIV), were run on *G. italicus* dataset. LDAs were cross validated through jackknife resampling.

RESULTS

General morphology.—Detailed morphological description of adults and nymphal instars and their measurements of *G. italicus* was provided by Gardini et al. (2017). For a better understanding of the following analyses, mean measurements and morphology of all body parts in each instar are shown in Table 1 and Figs. 1–31 respectively. During the post embryonic growth, linear increments of length measurements—expressed as percentage—describe the increment in size between two sequential instars. For each set of variables, it is possible to observe how differently each region grows; highest size increments characterize the last molt that leads from tritonymph to female for all regions (Fig. 32). Appendages (PC, LI and LIV) show a similar pattern, while within the UB region relative increment progressively decreases from protonymphs to males. When measurements related to width are considered, tritonymph to female increments turn out to be the highest again (Fig. 32). On the other hand, the last stage from tritonymph to male, shows increments close to those recorded in previous instars.

Testing trichobothrial positions.—The calculated increments of distances from the finger-tip, for three trichobothria are present beginning with the protonymphal instar, show a clear pattern: *ist* and *et,* located near the tip of the chela fixed finger, both feature mostly negative absolute values and this indicates a clear movement towards the distal end of the chela. Their values are from protonymph to deutonymph –0.0016 mm for *et* and –0.0015 mm for *ist*; deutonymph to tritonymph 0.0039 mm for *et* and 0.0150 mm for *ist*; tritonymph to male –0.0044 mm for *et* and –0.0112 mm for *ist*; tritonymph to female 0.0113 mm for *et* and 0.0131 mm for *ist*. These movements are even more clear when such increments are expressed as percentage (trichobothrial ratios): values of elements proximal to the end of the chela (*et* and *ist*) show negative values decreasing from –6.01% (protonymph to deutonymph) to –1.16% (tritonymph to females) for *et* and from –11.09% to –1.09% for *ist* in the same stages. Trichobothrium *eb* increments feature all positive values both in absolute and percentage terms, describing a movement towards the basal portion of the chela.

During the whole post embryonic development, the distance from the tip of the chela of trichobothrium *eb* (dfe series) increases considerably in all instars (Anova; $P = < 0.0001$, $F = 506.9$ with 4 and 45 df) pointing out a clear elongation of the chelal axis. Trichobothria *ist* and *it* – both located in the distal area of the chelal axis – show differences only when females are compared to nymphal instars. On the contrary, *ist* position in males is comparable with that of previous instars (Kruskal-Wallis test: chi-squared = 32.183, df = 4, $P = < 0.0001$, Fig.

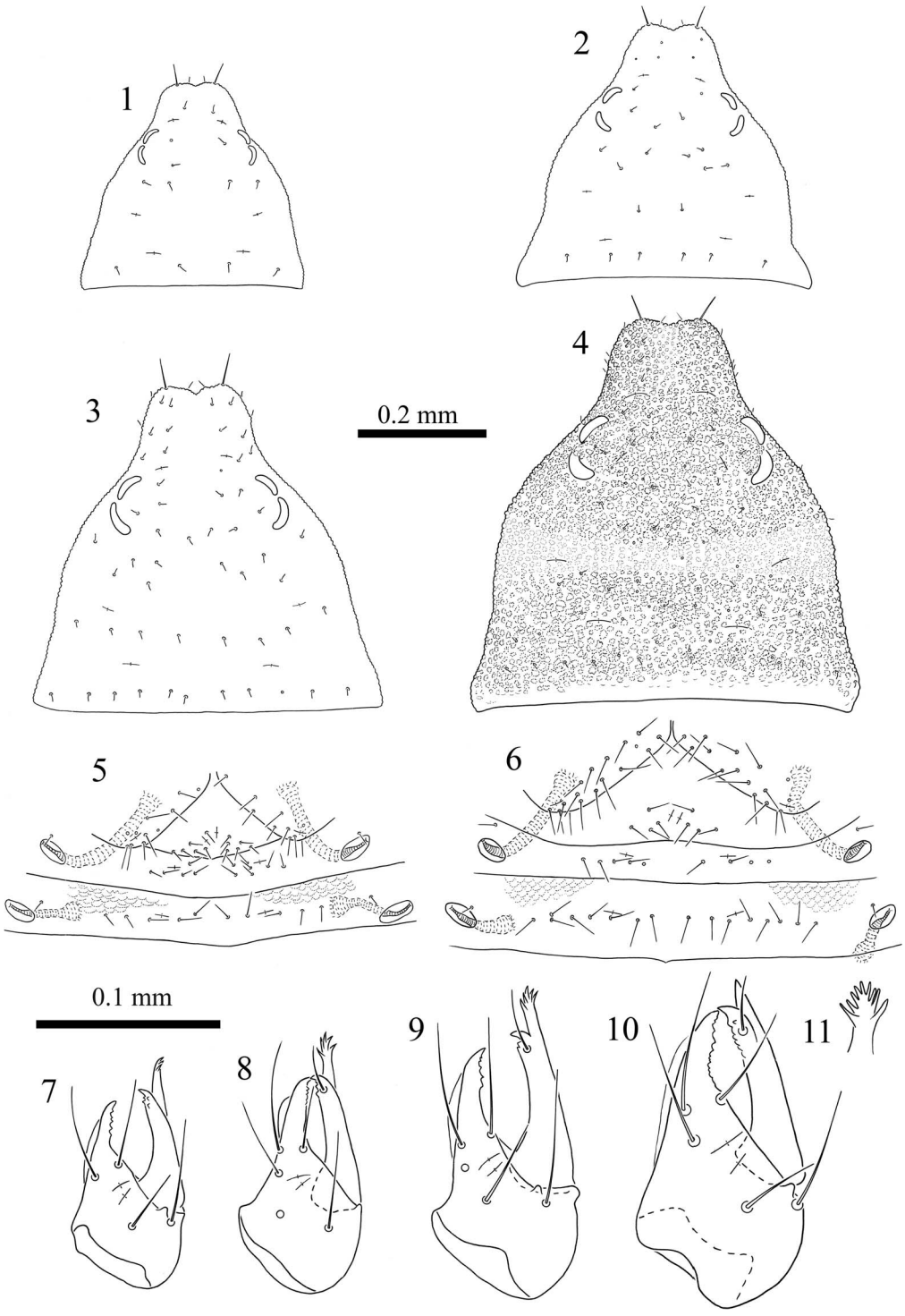

Figures 1–11.—*Geogarypus italicus* Gardini et al., 2017; 1, Carapace, dorsal, protonymph; 2, Carapace, dorsal, deutonymph; 3, Carapace, dorsal, tritonymph; 4, Carapace, dorsal, male [from Gardini et al., 2017]; 5, Sternites II–IV, male [from Gardini et al., 2017]; 6, Sternites II–IV, female [from Gardini et al., 2017]; 7, Chelicera, dorsal, protonymph; 8, Chelicera, dorsal deutonymph; 9, Chelicera, dorsal, tritonymph; 10, Chelicera, dorsal male [from Gardini et al., 2017]; 11, Galea, female [from Gardini et al., 2017].

33). Trichobothrium *ist* shifts to a more distal position in females, while in male specimens it shows an opposite trend going toward the base of the chela. Trichobothrium *it* is closer to *ist* in males than in females (Fig. 33).

Trichobothrium *et,* the closest to the finger-tip, significantly changes between protonymph and female, deutonymph and female and between sexes when absolute positions are compared (Kruskal-Wallis test: chi-squared = 30.17, df = 4,

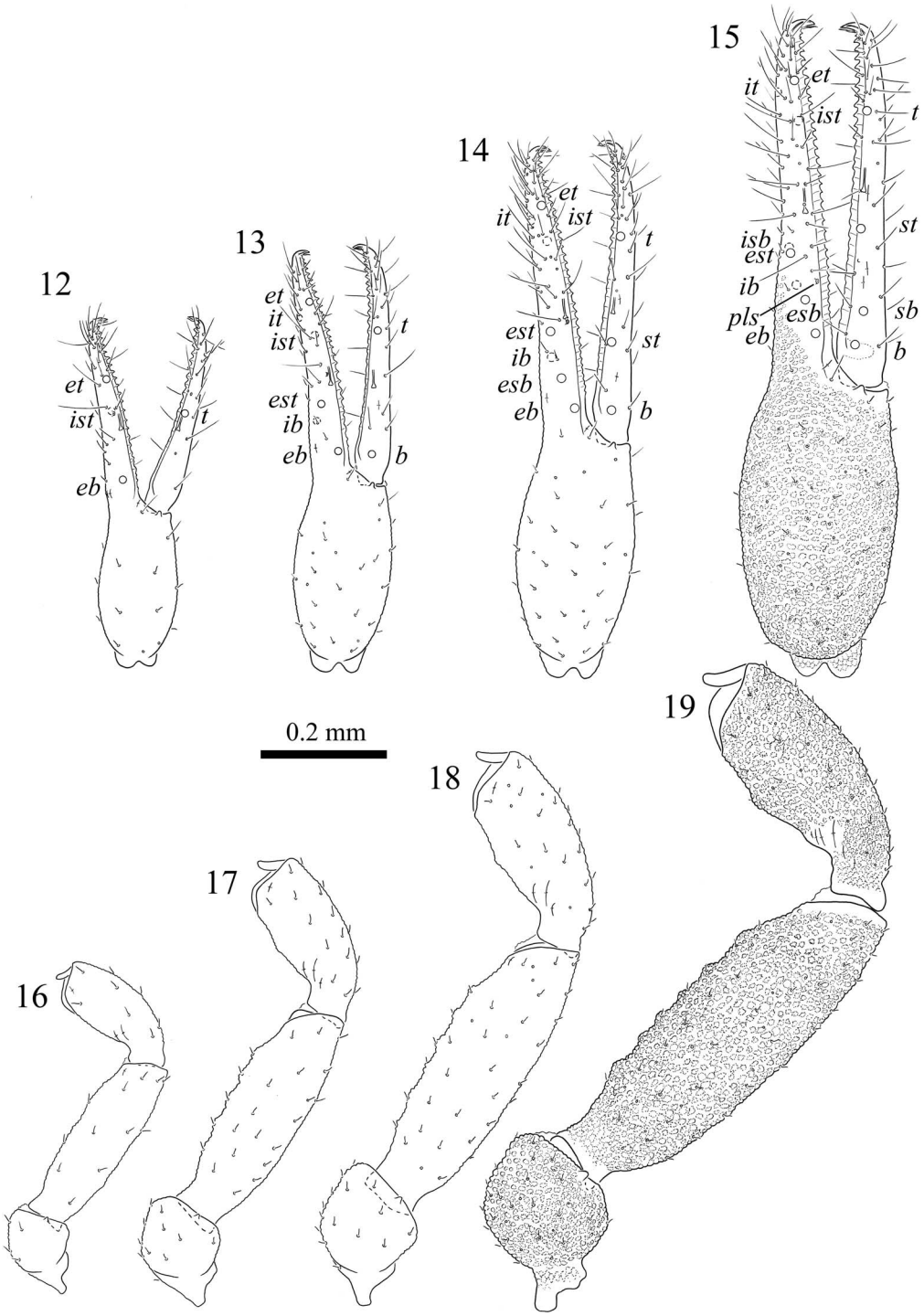

Figures 12–19.—*Geogarypus italicus* Gardini et al, 2017; 12, Right chela, lateral (granulation omitted), protonymph [from Gardini et al., 2017]; 13, Right chela, lateral (granulation omitted), deutonymph [from Gardini et al,2017)]; 14, Right chela, lateral (granulation omitted), tritonymph [from Gardini et al., 2017]; 15, Right chela, lateral, male [from Gardini et al., 2017]; 16, Right trochanter, femur and patella, dorsal (granulation omitted), protonymph; 17, Right trochanter, femur and patella, dorsal (granulation omitted), deutonymph; 18, Right trochanter, femur and patella, dorsal (granulation omitted), tritonymph; 19, Right trochanter, femur and patella, dorsal, male [from Gardini et al. 2017)].

$P = < 0.0001$). These results depict some degree of growth also in this apical portion of the axis.

Considering trichobothrium *t* on the movable finger, Dunn's test shows significant differences between the earlier stage and adults of both sexes but not between the last nymphal stage and the adults (Kruskal-Wallis test; chi-squared = 26.991, df = 4, $P = < 0.0001$, Fig. 33). Trichobothrial ratios of *et* (external margin of fixed finger), *ist* (internal margin of fixed finger) and *t* (terminal part of movable finger) decrease during growth (Figs. 33, 34, Table 2):

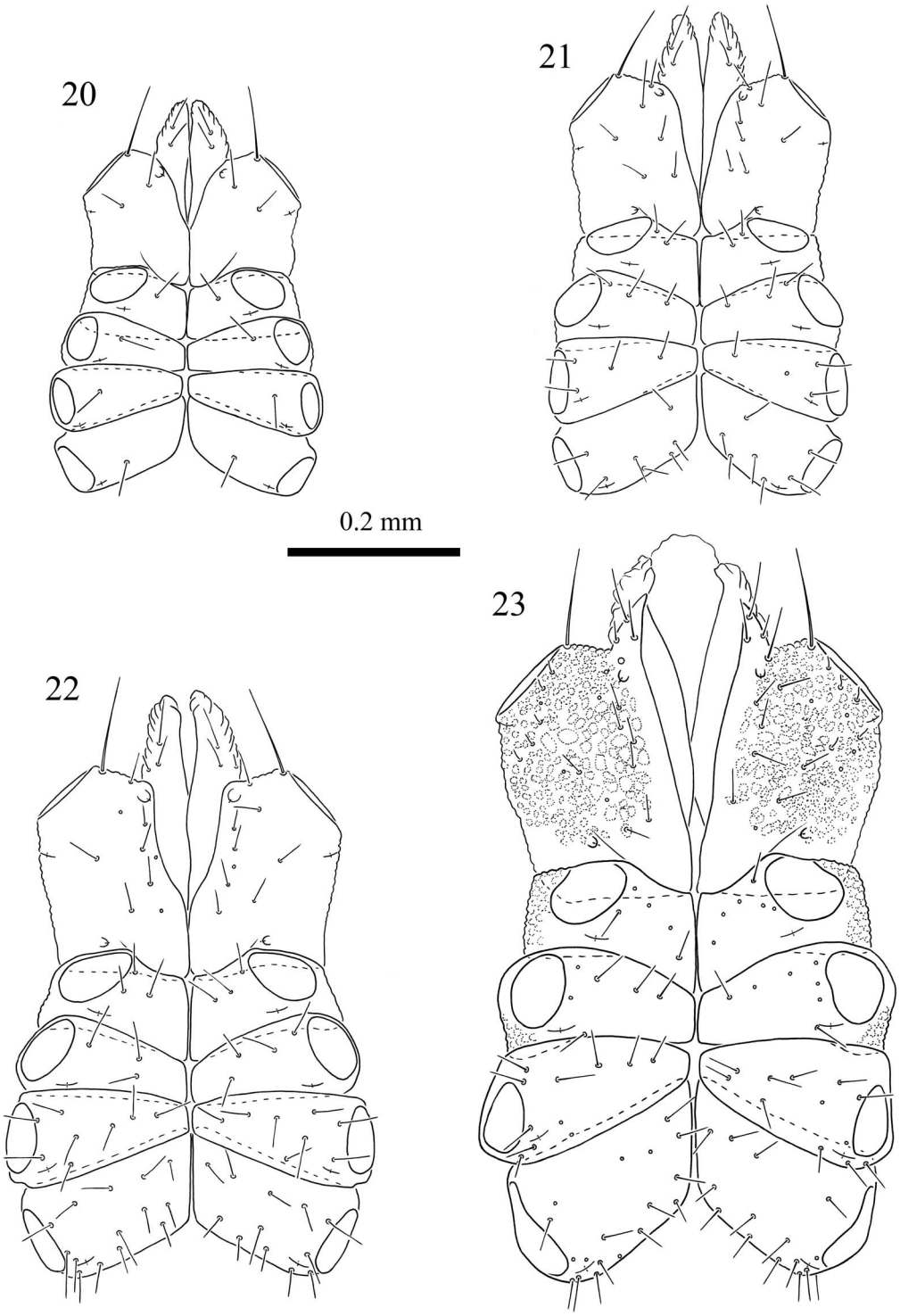

Figures 20–23.—*Geogarypus italicus* Gardini et al., 2017; 20, Coxal area, ventral (granulation omitted), protonymph; 21, Coxal area, ventral (granulation omitted), deutonymph; 22, Coxal area, ventral (granulation omitted), tritonymph; 20, Coxal area, ventral, male [from Gardini et al. 2017)].

this suggests that they are shifted to more distal positions. Dunn's test for trichobothrial ratios of *et*, *ist* and *t* shows overall significant differences for all instars (Kruskal-Wallis: chi-squared = 46.144, df = 4, $P = < 0.0001$; Kruskal-Wallis: chi-squared = 45.537, df = 4, $P = < 0.0001$; Anova: $P = <$ 0.0001, F = 506.9 with 4 and 45 df, Fig. 33). Trichobothrial ratios for trichobothrium *b* show a consistent higher value in females compared to males indicating a more proximal placement in females. Trichobothrial ratios for trichobothrium *b* show differences limited to the adult stages (Anova: P

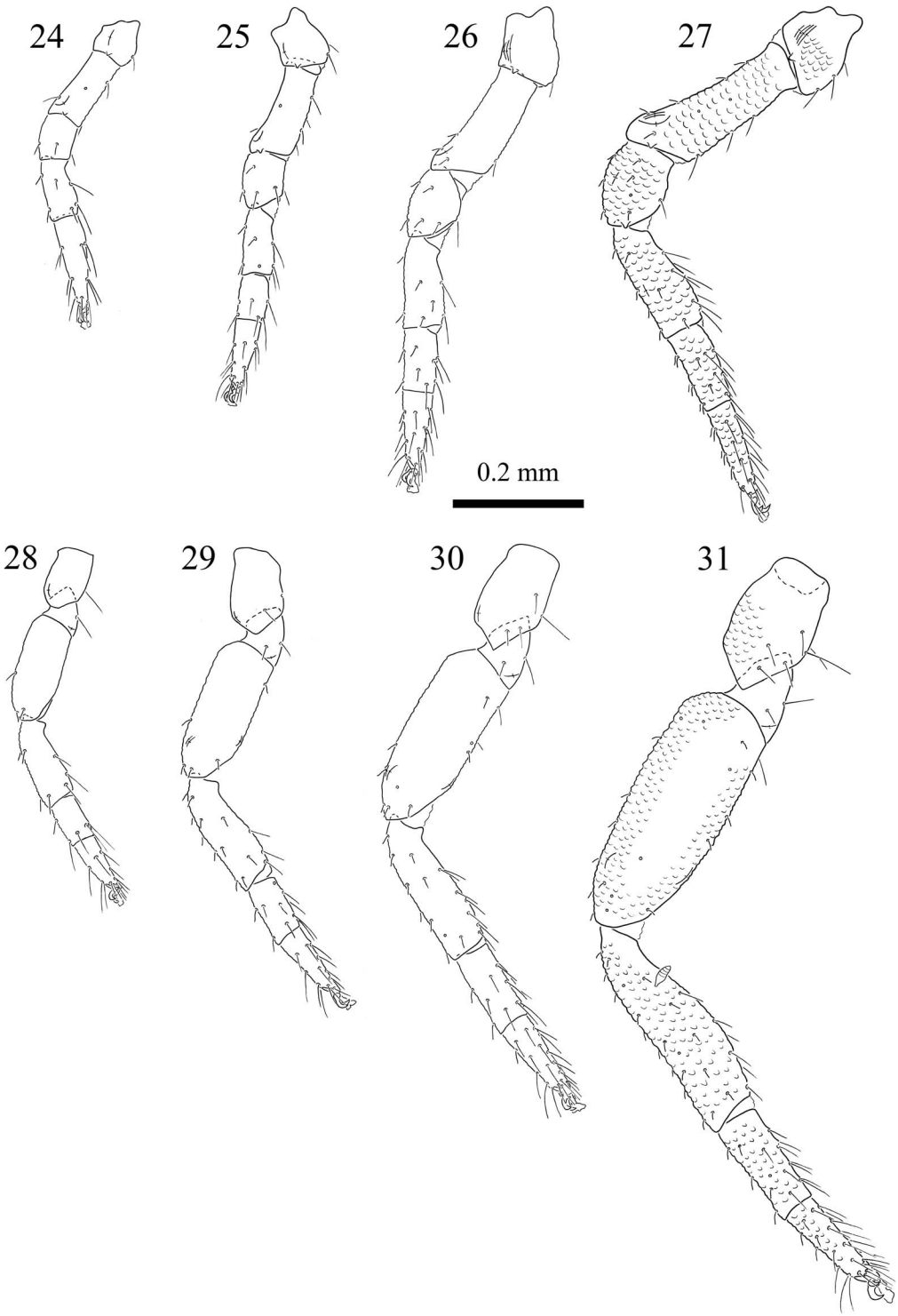

Figures 24–31.—*Geogarypus italicus* Gardini et al., 2017; 24, Right leg I, lateral, protonymph; 25, Right leg I, lateral, deutonymph; 26, Right leg I, lateral, tritonymph; 27, Right leg I, lateral, male [from Gardini et al. 2017)]; 28, Right leg IV, lateral, protonymph; 29, Right leg IV, lateral, deutonymph; 30, Right leg IV, lateral, tritonymph; 31, Right leg IV, lateral [with *Amphoromorpha* sp. (Zygomycota) on tibia], male [from Gardini et al. 2017)].

< 0.01, $F = 6.331$, with 3 and 36 df). When *eb* – located in the basal portion of the chela – is analysed in relative terms only female values differ from other instars (see Table S1, online at https://doi.org/10.1636/JoA-S-21-075.s1).

Chelal axis growth.—All the fitted regressions were good representations of data (Table 3). Slope values range from 1.1657 to 1.2685. All slope tests against the null hypothesis of isometric growth retrieve significant values, indicating that an

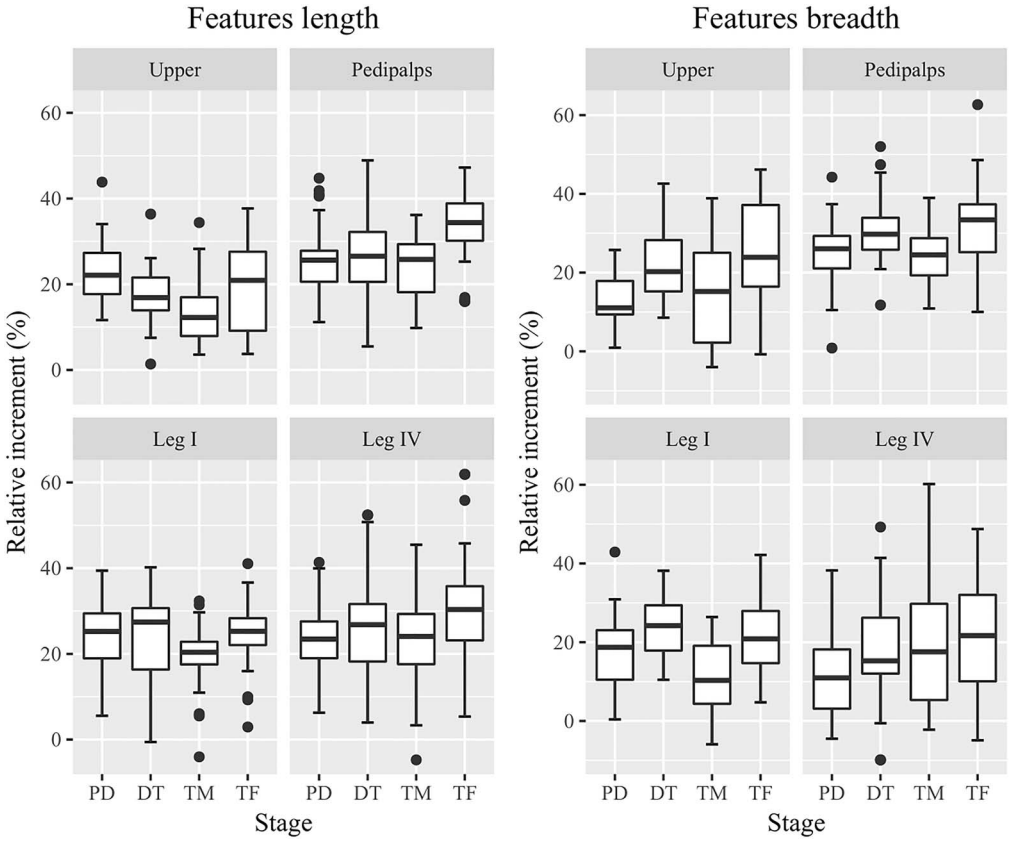

Figure 32.—*Geogarypus italicus* Gardini et al., 2017; Relative increment (expressed as percentage) of analysed body parts grouped by region and stage for length (left) and width (right) data. Outlyers are indicated as dots above and/or below the variation interval.

allometric process occurs in all stages (Table 3). Since the lines have been fitted through origin to the point ($b_{(n-1)}$, $b_{(n)}$), as described in Gabbutt (1969, 1972), their coefficient represents the growth rate of the chelal axis. The comparison of these values among stages through pairwise comparison against the null hypothesis of constant slope during the whole postembryonic growth (Table S2, online at https://doi.org/10.1636/JoA-S-21-075.s1) showed that the stage protonymph to deutonymph has higher coefficient than the tritonymph to male ($P < 0.02$, LRT = 8.4087) as well as the transition between deutonymph to tritonymph and tritonymph to male ($P < 0.02$, LRT = 8.0186). The values of the regression within tritonymph and females are higher (even though not significantly) than the tritonymph to male stage and they're closer to previous stages. The average increments (Table 4) calculated along the chelal axis in two successive stages are: from protonymph to deutonymph 0.0730 mm; deutonymph to tritonymph 0.0889 mm; tritonymph to female 0.0972 mm; tritonymph to male 0.0724 mm; total protonymph to male 0.2343 mm; total protonymph to female 0.2591 mm. In terms of percentage, lower growth values come from the tritonymph to male molt (16.93%,) while highest values were calculated for the deutonymph to tritonymph stage (26.86%). Linear increments within stages are quite different for almost all compared instar couples: females absolute increment is higher compared to males ($W = 20$, $P < 0.02$). The couples of instars protonymph-deutonymph and tritonymph-male ($W = 85$, $P < 0.01$), deutonymph to tritonymph and tritonymph-male ($W = 83$, $P < 0.05$) and finally tritonymph-male and tritonymph-female ($W = 23$, $P < 0.05$) all show statistically significant differences in their relative increment. The overall absolute and relative increments differ significantly between protonymph to male and protonymph to female. This result clearly underlines a differential growth of the chelal axis in reaching the adult size (absolute: $W = 11$, $P < 0.01$; relative: $W = 19$, $P = 0.02$).

Growth models.—Fitted regressions all give a good representation of data (Table 5, Figs. 34 a–d). The estimated slope values of males decrease as nymphs achieve maturity going from 1.2785 for tritonymph/male transformation to 1.5858 for the passage between protonymph/deutonymph. The coefficient related to the transformation of deutonymph/tritonymph is closer to the one characterizing the tritonymph becoming male (Bartlett-corrected likelihood ratio statistic testing for common slope: 1.38, $P = 0.8$) while it's higher in the molt from tritonymph to female (TF = 1.4076).

The middle growing region (MGR, Fig. 35) reaches its maximum extension in the molt from tritonymph to male (0.2707 mm; Fig. 35a, Table 5), while its maximum increase is achieved in the transition from deutonymph to tritonymph when the extension of this portion increases by 0.1313 mm. The non-growing portion of the chelal axis accounts for 54.31% in the first stage (protonymph to deutonymph) while it reaches its minimum in the following stage (Table 5, Fig. 36b). Higher values of non-growing area are achieved by the non-growing distal regions compared to the proximal one.

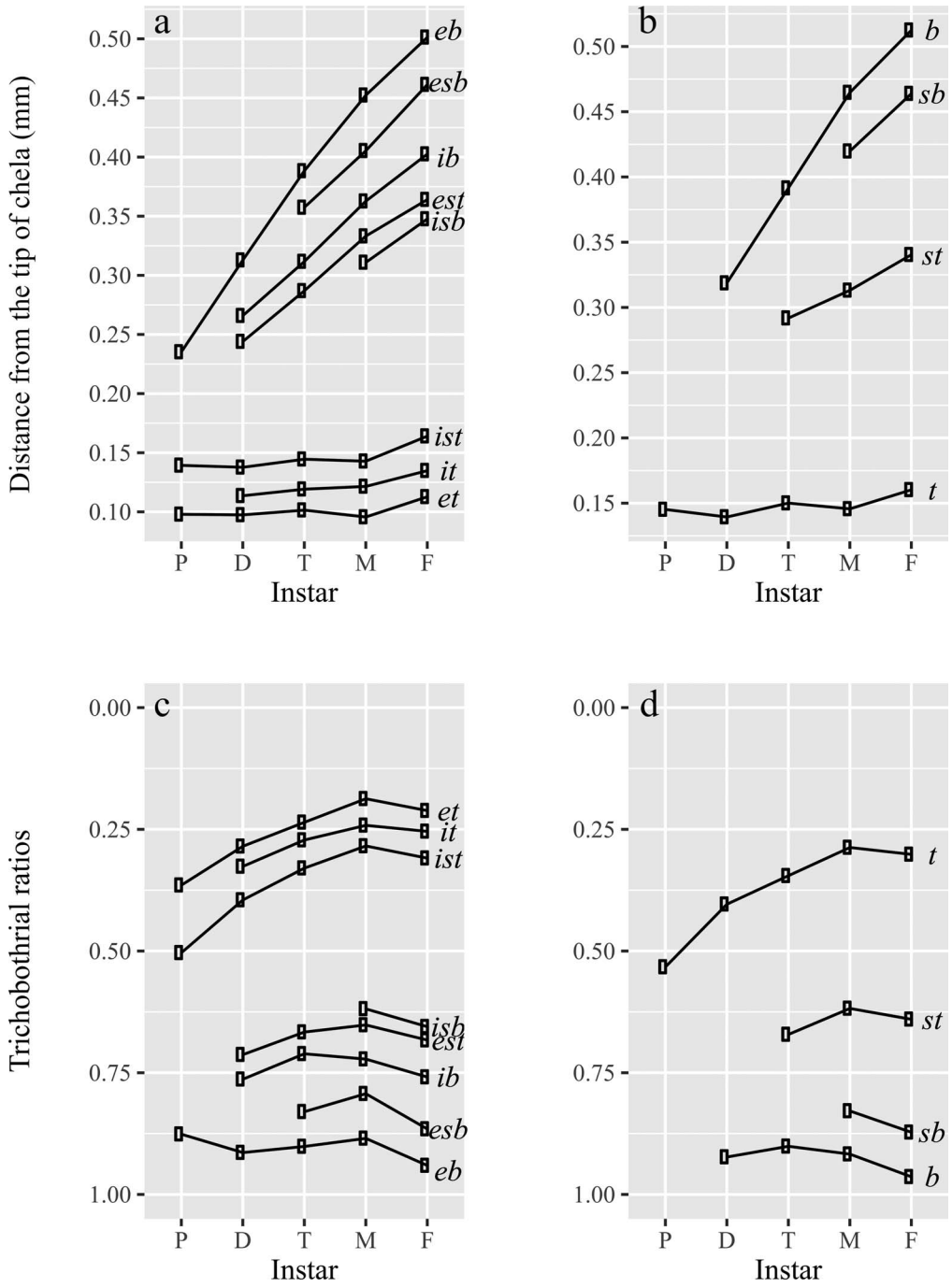

Figure 33.—*Geogarypus italicus* Gardini et al., 2017; Trichobothria absolute positions along the chelal axis plotted separately for fixed (a) and movable finger. (b); corresponding trichobothria are connected. Trichobothria relative positions along the chelal axis plotted as trichobothrial ratios separately for fixed (c) and movable finger (d); corresponding trichobothria are connected.

Although some minimal variations occur among instars, the absolute length of distal non-growing region (DNGR) remains approximately constant throughout the post-embryonic process. The length of the DNGR calculated according to the previous models is always greater than the proximal non-growing region (PNGR).

As consequence of this asymmetry the center of the growing region is proximally displaced from the middle of the chelal axis. Its absolute values are quite constant within all considered molts: PD = 0.0428 mm, DT = 0.0469 mm, TM = 0.0491 mm and TF = –0.0111 mm. Therefore, stages can be ranked from the lowest to highest value of relative proximal displacement: TF, TM, DT and PT with values of –2.55, 11.30, 13.57, 15.69 respectively.

Testing models.—The results of Wilcoxon Mann-Whitney paired test performed to infer the reliability of the predictions of trichobothria positions based on the Gabbutt (1972) formula are quite heterogeneous, evidencing in some cases

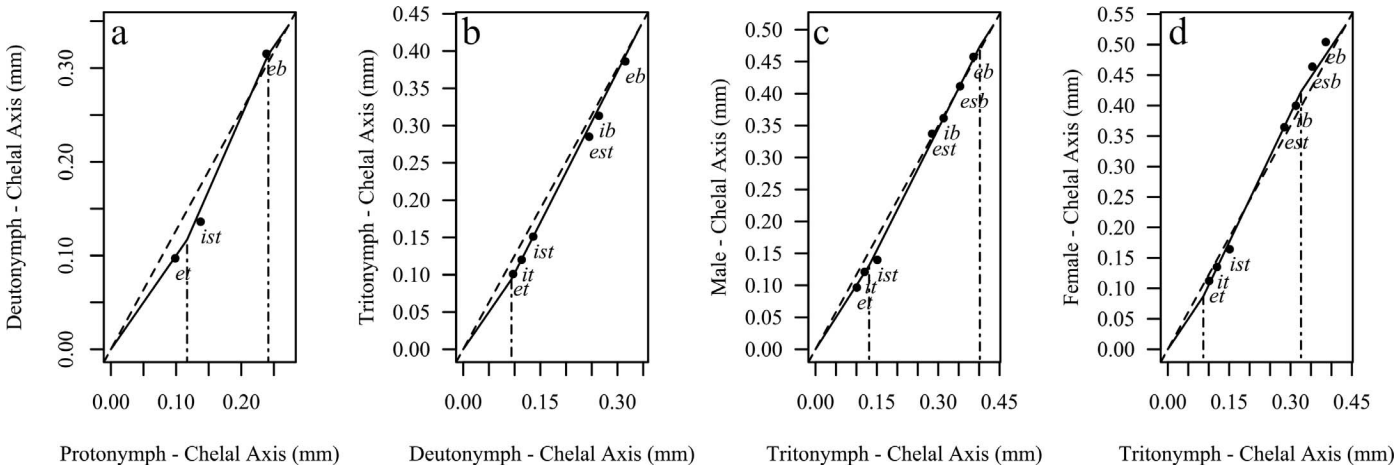

Figure 34.—*Geogarypus italicus* Gardini et al., 2017; trichobothrial regressions: the distances of trichobothria from the distal end of the chelal axis of each instar are plotted against those recorded in the following instar for protonymph to deutonymph (a), deutonymph to tritotonymph (b), tritotonymph to male (c) and tritotonymph to female (d). The calculated regression intersects the $y = x$ line drawn from the origin and from the point $b_{(n-1)}$, $b_{(n)}$. For further details see text.

relevant differences (Table S3, online at https://doi.org/10.1636/JoA-S-21-075.s1): the minimum mean estimation error (calculated as percentage) comes from tritonymph *it* (–1.00%, Table S4, online at https://doi.org/10.1636/JoA-S-21-075.s1), while the highest estimation error (41.15%) was calculated for trichobothrium *et* in female instar. Most differences in estimating trichobothria positions come from comparing *et* and *it* for which the error becomes highly significant compared to other trichobothria (Table S4).

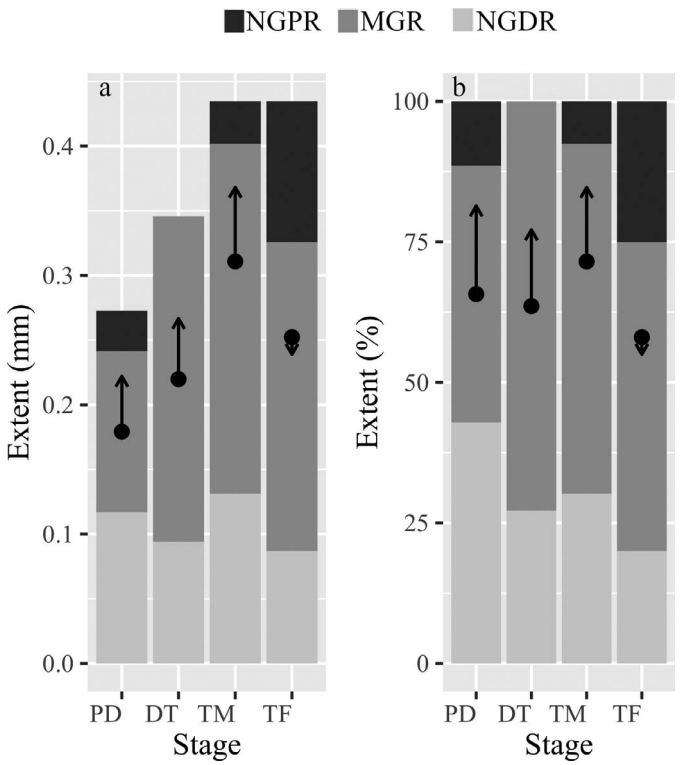

Figure 35.—*Geogarypus italicus* Gardini et al., 2017; the extent of growing region (MGR), non-growing distal region (NGDR) and non-growing proximal region (NGPR) calculated for each couple of instars both in absolute (a) and relative terms (%) (b). PD = protonymph to deutonymph, DT = deutonymph to tritonymph, TM = tritonymph to male, TF = tritonymph to female. Black point = center of the growing region from the tip, arrows = proximal displacement of the center of the growing region.

Growth rates and increments.—Since trichobothria are progressively added to the chelal axis as the individual reaches maturity, comparisons are possible only for the apical and basal portion of the chelal axis, limited by *et* (tip–*et* for the apical portion) and *eb* (*eb* – base for the basal portion). The ratios between the distance tip–*et* calculated for tritonymph to male and tritonymph to female are higher when compared to previous steps (Fig. 36). The same observation can be made for the axis portion comprised between the most basal trichobothrium and the base of the axis (*eb*–base). The mean chelal axis length for protonymphs (0.2727 mm), deutonymphs (0.3457 mm) and tritonymphs (0.4346 mm) allows to understand how growth occurs. The chelal axis absolute increment between protonymph and deutonymph is 0.0730 mm. The observed growth rates over the protonymphal axis are as follows: tip–*et*, 0.9855; *et*–*ist*, 1.0079: *ist*–*eb* 1.7837 and *eb*–base, 0.9046. The increments produced for the same portions from protonymph to deutonymph are –0.0016, 0.0001, 0.1401, and –0.0036 mm. Therefore, the increment of 0.0783 mm that occurs between the trichobothria *et* and *eb* is obtained from the sum of the previous values. The ratio between 0.0783 and 0.0730 returns a relative increment (expressed as percentage) of 107.26 %, pointing out a distance greater than that between the trichobothria *et* and *eb* (that correspond to the 100 %). Moreover, the estimated growth rate represented by the regression slope is 1.5859 (Table 5) and can be applied on a portion of chelal axis shorter than the distance between *et* and *eb* (Fig. 36a). For deutonymph to tritonymph, the axis increment is 0.0939 mm with an *et*–*eb* increment of 0.0670 mm, a distal increment (tip–*et*) of 0.0039 mm (4.15% of the total increment) and a proximal one (*eb*–base) of 0.0179 mm (19.06% of the total increment). In this case, the increment between *et* and *eb* (0.0670) represents 71.35% of the whole axis increment. The same estimation

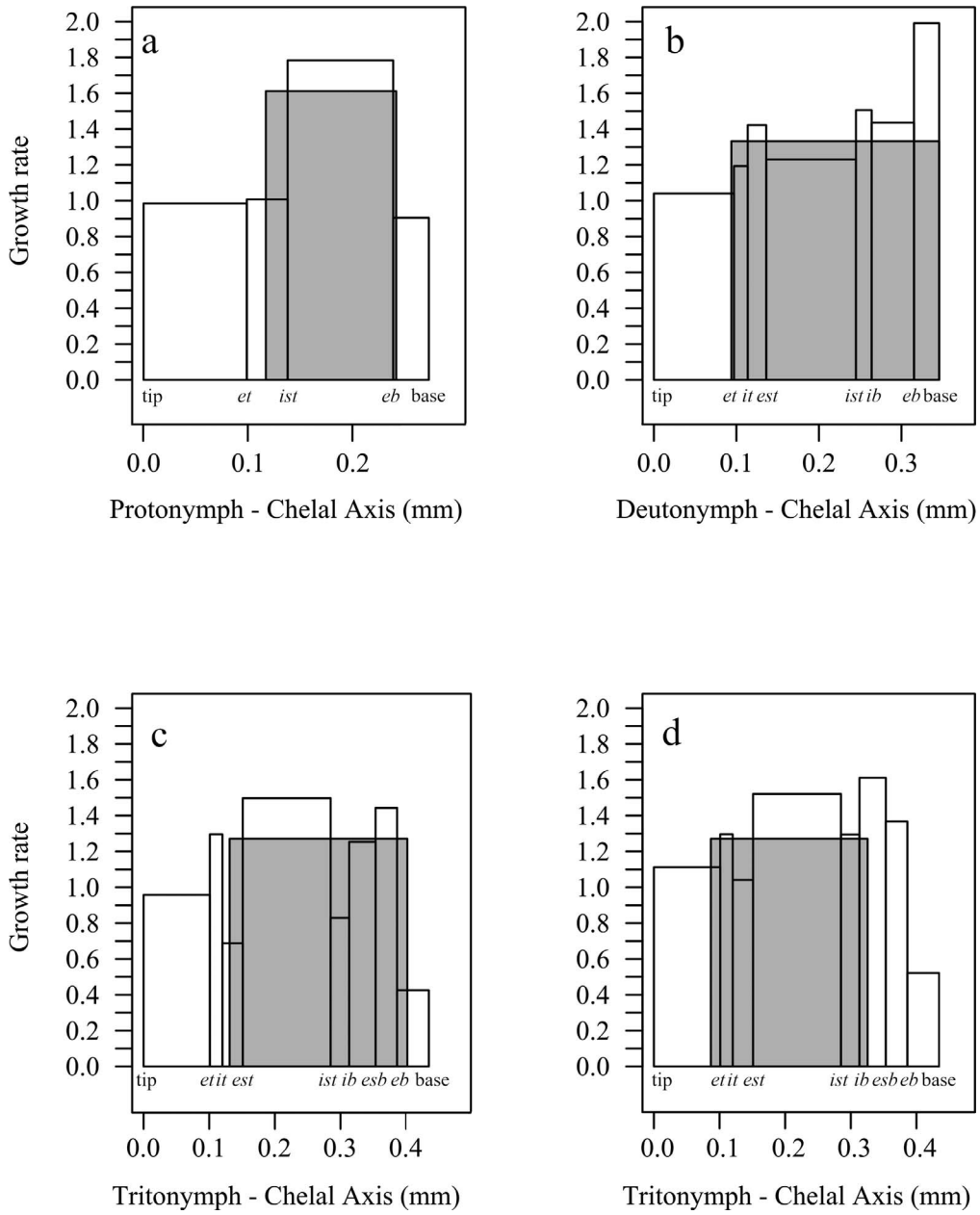

Figure 36.—*Geogarypus italicus* Gardini et al., 2017; the calculated growth rates between named trichobothria are plotted for (a) protonymph to deutonymph on the protonymphal axis, (b) deutonymph to tritonymph on the deutonymphal axis, (c) tritonymph to male on the tritonymphal axis and (d) tritonymph to female on the tritonymphal axis. The position and extent of the growing region and the growth rate as predicted from the models are represented by the grey area.

performed for tritonymph to male and tritonymph to female returns increments of 104.70% (0.0758 mm/0.0724 mm) and 113.07% (0.1068 mm/0.0724 mm) respectively. For these stages, fitted regression values operate very differently: while in male, the amplitude of the growing region (grey background, Fig. 36c) includes *eb* but not *et*, in females this region is shifted toward the tip of the axis, including *et* but not *eb*.

Ontogenetic allometry.—When protonymph to male regressions were considered, four models described an isometric growth (Table S5, online at https://doi.org/10.1636/JoA-S-21-075.s1) while most body parts showed a positive allometric growth with the only exception of leg I basitarsus, which shows a negative coefficient. This result can be easily understood with the following appearance of the telotarsus in the late stages. Highest slope values were achieved by smaller body parts such as chelicera width (1.7022) and leg IV basitarsus (2.1855). Females-related models revealed an isometric growth in more parts with particular reference to leg I features (Table S5). Basitarsus length of leg I follows the same pattern observed in male models. Most steep lines occur between basitarus and telotarsus width regressions while smallest slope is achieved by tibia length (0.8455). When the two groups of models are compared, only pedipalps related regression shows significant differences in growth values

Table 1.—*Geogarypus italicus* Gardini et al., 2017. Linear measurements (mean and standard deviation for 10 individuals of each lifestage). P, protonymph; D, deutonymph; T, tritonymph; M, adult male; F, adult female.

	P		D		T		M		F	
	mean	sd	mean	sd	mean	sd	mean	sd	mean	sd
Carapace										
Length	0.32	0.019	0.41	0.018	0.49	0.023	0.57	0.026	0.63	0.024
width	0.35	0.018	0.40	0.018	0.50	0.023	0.63	0.030	0.68	0.031
Cucullus length	0.08	0.009	0.11	0.004	0.15	0.006	0.18	0.007	0.21	0.007
Carapace furrow	0.12	0.003	0.15	0.004	0.17	0.008	0.18	0.002	0.18	0.003
Chelicera length	0.10	0.004	0.12	0.002	0.14	0.006	0.16	0.004	0.18	0.010
Chelicera width	0.06	0.004	0.06	0.003	0.07	0.004	0.08	0.003	0.08	0.005
Chelicera movable finger length	0.06	0.003	0.07	0.004	0.09	0.007	0.10	0.001	0.11	0.010
Pedipalps										
Trochanter length	0.12	0.004	0.16	0.008	0.19	0.014	0.23	0.007	0.25	0.006
Trochanter width	0.09	0.002	0.11	0.005	0.14	0.009	0.18	0.005	0.18	0.008
Femur length	0.28	0.006	0.34	0.009	0.45	0.022	0.57	0.010	0.61	0.021
Femur width	0.09	0.008	0.11	0.004	0.14	0.006	0.17	0.007	0.18	0.008
Patella length	0.19	0.011	0.23	0.006	0.30	0.017	0.38	0.009	0.40	0.008
Patella width	0.08	0.002	0.10	0.003	0.13	0.005	0.15	0.003	0.16	0.006
Chela with pedicel length	0.51	0.018	0.63	0.016	0.78	0.037	0.93	0.022	1.03	0.036
Chela without pedicel length	0.50	0.019	0.61	0.016	0.75	0.035	0.90	0.020	0.99	0.041
Hand with pedicel width	0.25	0.011	0.31	0.010	0.39	0.018	0.46	0.022	0.52	0.015
Hand width	0.13	0.007	0.16	0.005	0.21	0.010	0.26	0.009	0.29	0.016
Hand without pedicel length	0.23	0.010	0.28	0.008	0.36	0.021	0.42	0.028	0.47	0.026
Movable finger length	0.27	0.008	0.35	0.016	0.43	0.020	0.51	0.012	0.53	0.008
Leg I										
Trochanter length	0.06	0.003	0.08	0.002	0.09	0.007	0.11	0.002	0.11	0.003
Trochanter width	0.05	0.003	0.06	0.002	0.07	0.004	0.08	0.003	0.09	0.004
Femur length	0.10	0.006	0.12	0.005	0.16	0.005	0.19	0.002	0.20	0.008
Femur width	0.04	0.004	0.05	0.001	0.06	0.003	0.07	0.005	0.07	0.003
Patella length	0.06	0.004	0.07	0.001	0.10	0.005	0.11	0.003	0.12	0.004
Patella width	0.05	0.002	0.05	0.002	0.07	0.004	0.07	0.004	0.09	0.005
Tibia length	0.08	0.004	0.10	0.004	0.12	0.006	0.14	0.006	0.15	0.007
Tibia width	0.04	0.002	0.05	0.003	0.05	0.003	0.05	0.018	0.07	0.002
Basitarsus length	0.11	0.004	0.15	0.005	0.17	0.007	0.10	0.004	0.10	0.004
Basitarsus width	0.03	0.001	0.03	0.001	0.04	0.002	0.04	0.002	0.05	0.002
Telotarsus length							0.11	0.005	0.11	0.005
Telotarsus width							0.03	0.005	0.03	0.003
Leg IV										
Trochanter length	0.09	0.004	0.11	0.001	0.14	0.010	0.17	0.007	0.19	0.002
Trochanter width	0.06	0.003	0.07	0.001	0.09	0.007	0.12	0.005	0.12	0.003
Femur length	0.07	0.002	0.08	0.003	0.10	0.003	0.11	0.006	0.11	0.002
Femur width	0.05	0.004	0.05	0.003	0.06	0.004	0.08	0.005	0.08	0.002
Patella length	0.15	0.008	0.19	0.008	0.25	0.008	0.32	0.002	0.33	0.015
Patella width	0.06	0.003	0.07	0.004	0.09	0.006	0.11	0.005	0.12	0.004
Tibia length	0.13	0.005	0.16	0.008	0.21	0.010	0.26	0.005	0.28	0.014
Tibia width	0.05	0.002	0.05	0.002	0.06	0.003	0.07	0.002	0.08	0.003
Basitarsus length	0.07	0.003	0.09	0.005	0.11	0.007	0.14	0.002	0.15	0.007
Basitarsus width	0.04	0.002	0.04	0.004	0.05	0.002	0.05	0.001	0.05	0.003
Telotarsus length	0.08	0.004	0.10	0.005	0.11	0.005	0.13	0.007	0.15	0.008
Telotarsus width	0.03	0.002	0.03	0.002	0.04	0.002	0.04	0.002	0.04	0.003

Table 2.—The relationship between the distance of each trichobothrium from the finger tip (a_n) and the respective chelal axis (b_n) given as trichobothrial ratios in the protonymph (a_0/b_0), deutonymph (a_1/b_1), tritonymph (a_2/b_2), males (a_3/b_3), and females (a_4/b_4). Dashes indicate absence of a trichobothrium in a particular instar.

	et	*it*	*est*	*ist*	*isb*	*ib*	*esb*	*eb*	*t*	*st*	*sb*	*b*
P	0.3619	-	-	0.5050	-	-	-	0.8750	0.5325	-	-	-
D	0.2806	0.3289	0.7084	0.3937	-	0.7634	-	0.9118	0.4032	-	-	0.9219
T	0.2324	0.2763	0.6558	0.3477	-	0.7207	0.8132	0.8886	0.3454	0.6714	-	0.9008
M	0.2110	0.2540	0.6854	0.3088	0.6510	0.7518	0.8719	0.9539	0.3012	0.6401	0.8723	0.9637
F	0.1905	0.2391	0.6651	0.2759	0.6099	0.7134	0.8116	0.9026	0.2872	0.6176	0.8280	0.9166

Table 3.—Chelal axis regressions between successive instars ($b_{(n-1)}$, b_n). Estimated slope, lower and upper confidence interval of estimated slope, R^2, p-values and p-values of slope test against H_0 of isometric growth are shown. Est. = Estimated slope; Lo. CI = lower confidence interval of estimated slope, Up. CI = upper confidence interval of estimated slope; P <0.05 = *, P <0.01 = **.

	Length		Slope					Slope test	
	$b_{(n-1)}$	b_n	Est	Lo. CI	Up. CI	R^2	p-val.	Test val.	p-val.
P→D	0.2727	0.3457	1.2685	1.2226	1.3161	0.9976	4.10E-13**	1	2.18E-07**
D→T	0.3457	0.4346	1.2572	1.2247	1.2905	0.9988	1.91E-14**	1	1.57E-08**
T→M	0.4346	0.5070	1.1657	1.1176	1.2159	0.9969	1.38E-12**	1	2.74E-05**
T→F	0.4346	0.5318	1.2225	1.1853	1.2609	0.9983	8.53E-14**	1	2.12E-07**

between males and female (Mann Whitney: W = 8, p–value = 0.04).

When body regions (UB, PC, LI and LIV) are compared within sexes, UB showed higher values compared to other regions. Moreover, in females model growth values of PC region are higher compared to LI (Mann Whitney: W = 63, $P < 0.01$).

Size and proportions.—Linear discriminant analysis performed on all body regions separately, succeeded in discriminating different instars and adults according to ratio data. The highest overall accuracy has been achieved by leg IV (0.98), while lowest value belongs to pedipalps (0.56). In the first LDA, run on upper body ratio data (UB, Fig. 37a), the first two discriminant axis account for 96.82% of the overall trace (separation achieved by each discriminant function). While males and females overlap, protonymphs show consistent differences in term of upper body ratios. Despite the good amount of overall trace (91.39%), the second LDA (PC, pedipalps and chela ratio data, Fig. 37b) showed the lowest accuracy values: 20% of males were wrongly classified as tritonymphs, and 40% were included into females. Some tritonymphs (30%) have been misclassified as males.

In the analysis of leg I data (overall accuracy 0.90, 98.62% of the overall trace, Fig. 37c), deutonymphs and tritonymphs overlap while males and females turn out to be very different. The LDA run on leg IV data (LIV, 95.53% of the overall trace, Fig. 37d) highlights clear differences between nymphal instars and adults for the considered ratios.

DISCUSSION

The analysis of the life history of *Geogarypus italicus* confirms some hypotheses already suggested for other pseudoscorpion species but also offers interesting insight for future research.

The analysis of trichobothria positions (Figs. 33a, b) showed how their distance from the finger-tip changes: the distances of the apical trichobothria (*et, it* and *ist*) from the tip remain almost the same between instars while distances from the tip of basal ones such as *eb*, *isb* and *ib* increase. A more interesting overview comes from the study of relative position (Figs. 33c, d) that outline a bidirectional growth with *et*, *it* and *ist* moving distally as their ratios tend to zero, while ratios of trichobothria more distant from the fingertip show a different pattern, decreasing or remaining almost constant. When compared to other species, the change in terms of position of *ist* within *G. italicus* could be interpreted following the hypothesis introduced by Harvey (1992) to explain the positions of this trichobothrium together with *isb*. It appears also that elements proximal to the tip of the chela move independently from the trichobothria placed in the basal portion. In comparing the relative positions of *G. italicus* with other species like *Roncus lubricus* L. Koch, 1873 and *R. andreiini* (di Caporiacco, 1925) the most relevant feature is the ratio value of *est* that in *G. italicus* is closer to trichobothria placed in the basal portions such as *eb, esb* and *isb* while in both species of *Roncus* L. Koch, 1873, the value of the *est* ratio is comparable to the relative position of those trichobothria located in the apical portion of the chelal axis (Gabbutt & Vachon 1967; Gardini & Benelli 1991). The calculated ratios and increments clearly prove that the growth of the chelal axis does not occur evenly during the post embryonic process; for instance, in *G. italicus* differently from what was observed in other species (Gabbutt 1969), the basal and apical portions seem to undergo limited growth. This pattern can be only explained by a model based on growing regions opposed to non-growing ones. As matter of fact, trichobothria regressions all have steeper slopes compared to the lines that describe the sole growth of the chelal axis. The model proposed by Gabbutt (1969) seems to be reliable, with some limitations, in illustrating the post-embryonic growth of the chelal axis, which accounts for a middle growing region (MGR), a distal non-growing region (DNGR) and a proximal non-growing region (PNGR). From the analysis of the growing-non-growing regions, there are clear differences between the last molt that lead from tritonymph to male, on one side, and to female on the other: the relative amplitude of the non-growing proximal region in the latter is wider than those calculated from tritonymph to male. In observing the extent of the non-growing distal region, the situation is completely inverted with a narrower distal non growing region in the tritonymph to female stage. The calculated extent of the growing portion (expressed as %) is different when compared to values reported for the families Chernetidae, Cheliferidae and Neobisiidae (Gabbutt 1969, 1972; Gardini & Benelli 1991). However, the absolute length of the distal non-growing region (DNGR) of

Table 4.—Absolute, relative and relative percentage of mean increments of chelal axis in *Geogarypus italicus*. P, protonymph; D, deutonymph; T, tritonymph; M, adult male; F, adult female.

	Absolute	sd	Relative	sd	Relative(%)	sd
P→D	0.0889	0.01	0.2578	0.05	25.78	4.63
D→T	0.073	0.02	0.2686	0.07	26.86	6.55
T→F	0.0972	0.02	0.2258	0.05	22.58	5.52
T→M	0.0724	0.03	0.1693	0.07	16.93	7.15

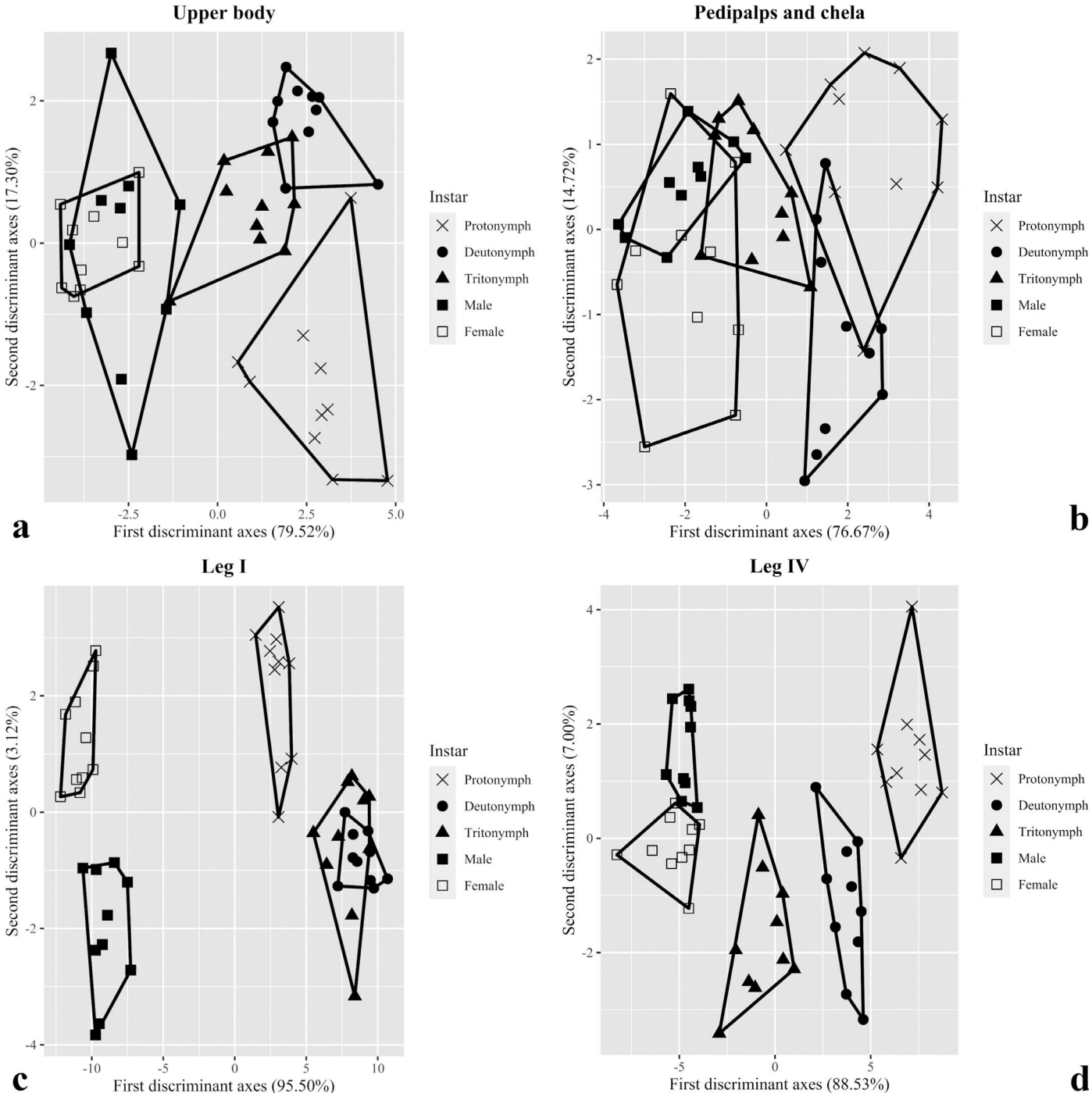

Figure 37.—*Geogarypus italicus* Gardini et al., 2017; Linear Discriminant Analysis (LDA) performed on ratio data for each body region.

G. italicus are comparable with those derived from studies on other species.

These values can be also interpreted by comparing the slopes of regression fitted to trichobothrial data: the slope values of *G. italicus* as well as those coming from regression related to neobisiid species (Gabbutt 1969) tend to decrease during the successive nymphal stages with the lowest rates being realized during the tritonymph/male transformation in *Neobisium maritimum* (Leach, 1817), *Neobisium carpenteri* (Kew, 1910) and *Roncus lubricus*. The same pattern can be observed in the chernetid species *Pselaphochernes dubius* (O. P.-Cambridge, 1892), *Dinocheirus panzeri* (C. L. Koch, 1836) and *Chernes cimicoides* (Fabricius, 1793). As in *G. italicus*, the highest growth rate is achieved from the deutonymph to tritonymph in *Neobisium muscorum* (Leach, 1817) Gabbutt 1969), *Allochernes wideri* (C. L. Koch, 1843), *Pselaphochernes scorpioides* (Hermann, 1804) and *Lamprochernes nodosus* (Schrank, 1803).

The passage from deutonymph to tritonymph is probably the most problematic to understand, because the regression

Table 5.—Trichobothria regressions and growth regions: correlation coefficient (R^2), p-values, degrees of freedom (df) and upper (Up. CI) and lower (Lo. CI) confidence interval. Non-growing proximal region (NGPR), middle growing region (MGR) and non-growing distal region (NGDR) are provided as absolute and relative percentage values. (P <0.05 = *, P <0.01 = **)

	Slope			Intercept						NGPR		MGR		NGDR	
	Esti.	Lo. CI	Up. CI	Est.	Lo. CI	Up. CI	R^2	p-val.	df	Abs	Rel	Abs	Rel	Abs	Rel
P→D	1.5859	1.5029	1.6734	-0.0685	-0.0835	-0.0536	0.9747	6.66E-02*	1	0.0312	11.44	0.1246	45.69	0.1169	42.87
D→T	1.3057	1.2798	1.3322	-0.0287	-0.0349	-0.0225	0.9873	3.66E-08**	5	0.0000	0.00	0.2518	72.84	0.0939	27.16
T→M	1.2786	1.2417	1.3166	-0.0366	-0.0465	-0.0266	0.9730	1.73E-07**	5	0.0328	7.55	0.2707	62.29	0.1311	30.17
T→F	1.4077	1.3795	1.4364	-0.0355	-0.0432	-0.0279	0.9769	2.17E-08**	5	0.1090	25.08	0.2388	54.95	0.0868	19.97

fitted among trichobothria fails to intercept any other line in the distal portion of the chelal axis, the model needs to be refitted using the finger-tip as a point of intersection. This feature was already observed by Gabbutt (1972). Under this assumption no distal non-growing region exists within certain circumstances. This feature is shared by *G. italicus*, *Roncocreagris cambridgei* (L. Koch, 1873) and *P. dubius*. Thus, there are differences in the slope values of trichobothria regressions among families but also within species. However this observation must be treated with caution since data are available for just a few species. It is more likely that different slopes may be also related to different ecological features which may favor some growth strategies more than others.

In all the stages, the increments of the ratio between the portion from the first to the last trichobothria (*et* and *eb*, respectively) and the whole chelal axis as a percentage were greater than the increment between the trichobothria and the increment of the chelal axis itself. These results provide another dissimilarity to the observations by Gabbutt (1970b) for *Dactylochelifer latreillii* (Leach, 1817) for which these values were somehow constant among stages and the growing region included all of the area involved in the increment process. This difference may imply that, independently from regression slopes, the way in which each portion contributes to the overall chelal growth can be more related to taxonomic proximity.

The only hypothesis available for *G. italicus* is the assumption that both the non-growing proximal and distal regions play a role in the growth of the chelal axis as demonstrated by the growing rate of the chelal axis portions (Fig. 36).

The reliability of the Gabbutt (1972) model in predicting the trichobothrial positions needs to be better investigated within more species across a broader taxonomic range, since chelal growth may follow different patterns in different families which may sometimes also include differential trichobothrial migration (Harvey 1992).

The different patterns of growth in each portion of the chelal axis as well as in trichobothrial positions can be partly explained by the phylogeny proposed by Benavides et al. (2019) that place *Geogarypus* in a different clade (Panctenata) from Neobisiidae (Hemictenata) and includes Cheliferidae in the infraorder Elassomatina. However, to understand these processes further analyses on more taxa are required. The study of ontogenetic allometry has revealed a clear sexual dimorphism, which is a quite common feature among arachnids in general (McLean et al. 2018) and also among pseudoscorpions in particular (Zeh 1987; Palen-Pietri et al. 2019). The dimorphism in pedipalpal features may be driven by the fighting behaviour of males. The bigger pedipalpal features of females may be related to the handling of the egg-pouch (Andrade & Gnaspini 2003) as described for *Maxchernes iporangae* Mahnert & Andrade, 1998, while it's not likely related to mating behaviour since geogarypids are known to be among non-pairing species (Harvey 1992; Choe & Crespi 1997). Absolute differences in pedipalpal chelae could be primarily due to the overall difference in body size between sexes, with females larger than males.

The analyses performed on the trichobothrial positions on the chelal axis data, as well as the allometric allocation and the ratio analyses, show the existence of a differential growth process that leads to sexually dimorphic adults, as already postulated for other arachnids (Buzatto & Machado 2014). To date, no other comparisons are available for pseudoscorpions as the current work is the first that has analysed the whole growth process of a single species but not limited to the pedipalpal chela.

Further analyses will undoubtedly help to understand if the differences in the growth patterns observed between pseudoscorpion taxa at higher taxonomical levels may be related to their phylogenetic heritage.

ACKNOWLEDGMENTS

The authors would like to thank the anonymous reviewers for their insightful comments and valuable suggestions that helped greatly improve the manuscript. We would also like to acknowledge the late Peter D. Gabbutt and Max Vachon for their pioneering works without whom this paper would never have been possible.

SUPPLEMENTAL MATERIALS

The following files are available online at https://doi.org/10.1636/JoA-S-21-075.s1

Table S1.—Trichobothrial ratios: Tukey's HSD pairwise comparison after significant One-Way ANOVA between instars for several trichobothria.

Table S2.—The relationship between the distance of each trichobothrium from the finger tip (a_n) and the respective chelal axis (b_n).

Table S3.—Wilcoxon Mann-Whitney for paired samples between observed and predicted trichobothria values

Table S4.—The mean, minimum and maximum estimated position of each trichobothrium calculated by the formula proposed by Gabbutt (1969).

Table S5.—Ontogenetic allometry: regression fitted to data from protonymph to male.

LITERATURE CITED

Andrade R de, Gnaspini P. 2003. Mating behavior and spermatophore morphology of the cave pseudoscorpion *Maxchernes iporangae* (Arachnida: Pseudoscorpiones: Chernetidae). *Journal of Insect Behaviour* 16:37–48.

Blackith RE, Reyment RA. 1971. Multivariate morphometrics. Academic Press, London–New York.

Benavides LR, Cosgrove, JG, Harvey MS, Giribet G. 2019. Phylogenomic interrogation resolves the backbone of the Pseudoscorpiones tree of life. *Molecular Phylogenetics and Evolution* 139:106509.

Baur H, Leuenberger, C. 2011. Analysis of ratios in multivariate morphometry. *Systematic Biology* 60:813–825.

Buzatto BA, Machado G. 2014. Male dimorphism and alternative reproductive tactics in harvestmen (Arachnida: Opiliones). *Behavioural Processes* 109:2–13.

Canard A, Stockmann R. 1993. Comparative postembryonic development of arachnids. In: Proceedings of the XII International Congress of Arachnology. *Memoirs of the Queensland Museum* 33:461–468.

Chamberlin JC. 1931. The Arachnid order Chelonethida. *Stanford University Publications, Biological Sciences* 7:1–284.

Choe JC, Crespi BJ. 1997. The Evolution of Mating Systems in Insects and Arachnids. Cambridge University Press, Cambridge.

Dunn OJ. 1961. Multiple comparisons among means. *Journal of the American Statistical Association* 56:52–64.

Fox GA, Cooper AM, Hayes WK. 2015. The dilemma of choosing a reference character for measuring sexual size dimorphism, sexual body component dimorphism, and character scaling: cryptic dimorphism and allometry in the scorpion *Hadrurus arizonensis*. *PLoS One* 10(3):e0120392.

Gabbutt PD. 1965. The external morphology of two pseudoscorpions *Neobisium carpenteri* and *Neobisium maritimum*. *Proceedings of the Zoological Society of London* 145:359–386.

Gabbutt PD. 1969. Chelal growth in pseudoscorpions. *Journal of Zoology* 157:413–427.

Gabbutt PD. 1970a. Sampling problems and the validity of life history analyses of pseudoscorpions. *Journal of Natural History* 4:1–15.

Gabbutt PD. 1970b. The external morphology of the pseudoscorpion *Dactylochelifer latreillei*. *Journal of Zoology* 160:313–335.

Gabbutt PD. 1972. Differences in the disposition of trichobothria in the Chernetidae (Pseudoscorpiones). *Journal of Zoology* 167:1–13.

Gabbutt PD, Vachon M. 1965. The external morphology and life history of the pseudoscorpion *Neobisium muscorum*. *Proceedings of the Zoological Society of London* 145:335–358.

Gabbutt PD, Vachon M. 1967. The external morphology and life history of the pseudoscorpion *Roncus lubricus*. *Journal of Zoology* 153:475–498.

Gardini G, Benelli R. 1991. The external morphology of the pseudoscorpion *Roncus andreinii*. *Journal of Zoology* 223:27–48.

Gardini G, Galli L, Zinni M. 2017. Redescription of *Geogarypus minor*, type species of the genus *Geogarypus*, and description of a new species from Italy (Pseudoscorpiones: Geogarypidae). *Journal of Arachnology* 45:424–443.

Gnaspini P. 1995. Reproduction and postembryonic development of *Goniosoma spelaeum*, a cavernicolous harvestman from southeastern Brazil (Arachnida: Opiliones: Gonyleptidae). *Invertebrate Reproduction & Development* 28:137–151.

Gould SJ. 1966. Allometry and size in ontogeny and phylogeny. *Biological Reviews* 41:587–638.

Harvey MS. 1987. A revision of the genus *Synsphyronus* Chamberlin (Garypidae: Pseudoscorpionida: Arachnida). *Australian Journal of Zoology, Supplementary Series* 126:1–99.

Harvey MS. 1988. The systematics and biology of pseudoscorpions. Pp. 75–85. *In* Australian Arachnology. (A.D. Austin, N.W. Heather eds.) The Australian Entomological Society, Brisbane.

Harvey MS. 1992. The phylogeny and classification of the Pseudoscorpionida (Chelicerata: Arachnida). *Invertebrate Systematics* 6:1373–1435.

Hui W, Gel YR, Gastwirth JL. 2008. lawstat: an R package for law, public policy and biostatistics. *Journal of Statistical Software* 28(3):1–26.

Huxley J. 1932. Problem of Relative Growth. Methuen & Co., London.

Klingenberg CP, Zimmermann M. 1992. Static, ontogenetic, and evolutionary allometry: a multivariate comparison in nine species of water striders. *The American Naturalist* 140:601–620.

Mayr E, Ashlock OD. 1991. Principles of Systematic Zoology. McGraw-Hill College, New York.

McLean CJ, Garwood RJ & Brassey CA. 2018. Sexual dimorphism in the Arachnid orders. *PeerJ* 6:e5751.

Palen-Pietri R, Ceballos A, Peretti AV. 2019. Sexual dimorphism and patterns of sexual behavior in *Lustrochernes argentinus* (Pseudoscorpiones: Chernetidae). *Journal of Arachnology* 47:344–350.

Pohlert T, Pohlert MT. 2018. The pairwise multiple comparison of mean ranks package (PMCMR). *R package* 27(2020):10.

R CORE TEAM. 2017. R: a Language and Environment for Statistical Computing, version R-3.4. 1. Vienna, Austria: R Foundation for Statistical Computing.

Reiss MJ. 1991. The Allometry of Growth and Reproduction. Cambridge University Press, Cambridge.

Ripley B, Venables B, Bates DM, Hornik K, Gebhardt A, Firth D, et al. 2013. Package 'mass'. Cran R, 538.

Shea BT. 1985. Ontogenetic allometry and scaling. Pp. 175–205. *In* Size and Scaling in Primate Biology. Advances in Primatology (Jungers WL, ed.), Springer, Boston, MA.

Shingleton A. 2010. Allometry: the study of biological scaling. *Nature Education Knowledge* 3(10): 2.

Sivaraman S. 1982. Chelal growth in three species of South Indian pseudoscorpions and their taxonomic relevance. *Entomon* 7:187–195.

Sokal RR, Rohlf FJ. 1995. Biometry: the Principles and Practice of Statistics in Biological Research. W.H. Freeman & Co., New York.

Vachon M. 1936. Sur le développement post-embryonnaire des Pseudoscorpiones (4 ème note). Les formules chaetotaxiques des pattes-mâchoire. *Bulletin du Muséum National d'Histoire Naturelle, Paris* 8:77–83.

Warton DI, Weber NC. 2002. Common slope tests for bivariate errors-in-variables models. *Biometrical Journal: Journal of Mathematical Methods in Biosciences* 44:61–174.

Warton DI, Duursma RA, Falster DS, Taskinen S. 2012. smatr 3-an R package for estimation and inference about allometric lines. *Methods in Ecology and Evolution* 3:257–259.

Wickham H. 2011. ggplot2. *Wiley Interdisciplinary Reviews: Computational Statistics* 3:180–185.

Winston JE. 1999. Describing Species: Practical Taxonomic Procedure for Biologists. Columbia University Press, New York.

Zeh DW. 1987. Aggression, density, and sexual dimorphism in chernetid pseudoscorpions (Arachnida: Pseudoscorpionida). *Evolution* 41:1072–1087.

Manuscript received 26 November 2021, revised 9 July 2022, accepted 22 August 2022.